

# Study of Multiple Diffraction of X-rays in Perfect Crystals with the Use of Synchrotron Radiation<sup>1</sup>

A. Yu. Kazimirov\*, M. V. Koval'chuk\*, and V. G. Kohn\*\*

\**Shubnikov Institute of Crystallography, Russian Academy of Sciences, Leninskii pr. 59, Moscow, 117333 Russia*

\*\**Kurchatov Institute of Atomic Energy, pl. Kurchatova, Moscow D-182, 123182 Russia*

Received July 20, 1993

**Abstract** – The experiments on multiple diffraction of X-rays in perfect crystals performed with the participation of the authors are reviewed. The experiments include direct measurements of anomalous transmission of X-rays under the conditions of six-beam diffraction and the study of photoelectron yield under the conditions of three-beam diffraction (a multibeam modification of the method of X-ray standing waves). Various X-ray–optical arrangements for two-dimensional collimation, necessary for observation of multibeam interference effects, are analyzed. Sufficiently good agreement between the experimental and calculated data confirms the efficiency of the suggested solutions. These solutions are rather promising for the development of new non-destructive methods for analyzing structure perfection of crystals and surface layers.

## 1. INTRODUCTION

The dynamical theory of X-ray diffraction developed at the beginning of our century is an outstanding achievement of theoretical physics of that time. In essence, the theory reduces to a self-consistent allowance for the interaction of incident and diffracted X-ray waves and the formation, as a result, of a unified wave field in the crystal. The intensity of this field is space-modulated and repeats the periodic structure of the crystal lattice of a perfect crystal.

All of the interference effects of dynamical scattering of X-rays are directly related to the existence of this wave field and its interaction with the atoms of the crystal lattice. One of the main effects of this kind is anomalous transmission of X-rays and anomalous angular dependences of the yields of secondary radiations (photoelectrons, fluorescence, etc.). But the absence of sufficiently large perfect crystals hindered experimental study for decades of the effects predicted by the dynamical theory.

The synthesis of crystals with a high degree of perfection gave a new impetus to studies of dynamical effects in the simplest two-wave diffraction geometry, where the reflection conditions are fulfilled only for one system of crystallographic planes. As a result, new methods for structure diagnostics of almost perfect single crystals were developed, such as X-ray topography, diffractometry, and various modifications of the method of X-ray standing waves. The widespread use of these methods provided the improvement of modern technologies for growing various technically important crystals, especially those used in microelectronics.

Multiple diffraction is a more complex case, where the reflection conditions are fulfilled simultaneously

for two or more crystal planes. As a result, three and more strong beams propagating in different directions can arise in the crystal. The coherent superposition of these beams is responsible for the formation of a complex structure of the wave field, whose intensity is modulated in two directions. In principle, this provides better conditions for the manifestation of interference effects of X-ray scattering and their use for structure diagnostics. A detailed description of the various possible cases of multiple diffraction can be found in the fundamental work by Z.G. Pinsker [1].

The experimental study of the dynamical effects of multiple diffraction has been hindered for many years by a series of objective difficulties. First of all, it was necessary to collimate an incident X-ray beam simultaneously in two directions (the so-called two-dimensional collimation) with a high accuracy (of about 1"). In addition to the technical difficulties of its implementation, this collimation gives rise to a drastic decrease in intensities (by several orders of magnitude in comparison with two-wave diffraction). Second, the goniometric devices used should provide the precision rotations of the crystal about several (at least, two) axes. Therefore, it is not surprising that the experiments in this field became possible only recently mainly because of the use of intense synchrotron radiation (SR).

Below we briefly review the main experimental results obtained in our studies with the use of both conventional X-ray sources in the Laboratory of X-ray Optics and Synchrotron Radiation of the Institute of Crystallography of the Russian Academy of Sciences and also with the use of an SR source of the Photon Factory (Tsukuba, Japan). The experiments were performed with the participation of I.Yu. Kharitonov and L.V. Samoilova from the Institute of Crystallography and S. Kikuta and T. Ishikawa from the University of Tokyo [2 - 6].

<sup>1</sup>In memory of Z.G. Pinsker.

Section 2 is devoted to the consideration of the main equations of the multibeam dynamical theory of diffraction and the methods of their solution. The methods for solving the main problem of the multibeam X-ray experiment (two-dimensional beam collimation) are considered in Sect. 3. Section 4 deals with the results of the first diffractometric measurements of beam intensities in anomalous transmission of X-rays under the conditions of six-beam diffraction. For the first time, a rather good quantitative agreement is achieved between the experimental results and theoretical calculations.

The measurements of the yields of secondary radiations under the conditions of multiple diffraction (the multibeam modification of the method of X-ray standing waves) is an independent experimental problem. Section 5 deals with the first measurements of the photoelectron yield under the conditions of three-beam X-ray diffraction. We also describe the method for calculating the yields of secondary radiations in the multibeam geometry and compare the calculated and experimental data.

The main disadvantage of the conventional two-beam X-ray diffraction experiment is the loss of information on phases. The method of X-ray standing waves provides this information, but presents essential experimental difficulties associated with the necessity of measuring the yields of secondary radiations. Multiple diffraction allows the solution of the phase problem without the use of secondary processes. The optimum method for solving the phase problem for almost perfect single crystals is described in Section 6.

## 2. THEORY

The dynamical theory of X-ray diffraction was first developed as a phenomenological theory (the history of the problem is considered in detail elsewhere [1, 7]). Later, a rigorous theory was developed. It was described most consistently by Kagan and Afanas'ev [8]. The theory is based on the Maxwell equation for the electric-field amplitude  $\mathbf{E}(\mathbf{k}, \omega)$  of an X-ray wave in the reciprocal space, i.e.,

$$(k^2 - K^2) \mathbf{E}(\mathbf{k}, \omega) - \mathbf{k} [\mathbf{k} \cdot \mathbf{E}(\mathbf{k}, \omega)] = (4\pi i \omega / c^2) \mathbf{j}(\mathbf{k}, \omega), \quad (1)$$

where  $K = \omega/c = 2\pi/\lambda$ , and  $\lambda$  is the wavelength. The right-hand side includes the Fourier component of the induced-current density  $\mathbf{j}(\mathbf{k}, \omega)$  calculated rigorously as the quantum-mechanical average of the current-density operator over the crystal states in the radiation field. With due regard for a weak interaction of X-rays with the crystal, the second term in (1) (nontransversity) can be ignored; then, one can calculate the current in the approximation linear with respect to the field. In the general case, we obtain for a strictly periodic crystal

$$j^i(\mathbf{k}_0, \omega) = (c^2 K^2 / 4\pi i \omega) \sum_{mj} \chi_{\omega}^{ij}(\mathbf{k}_0, \mathbf{k}_m) E^j(\mathbf{k}_m, \omega), \quad (2)$$

where  $\mathbf{k}_m = \mathbf{k}_0 + \mathbf{h}_m$ ,  $\mathbf{h}_m$  is the  $m$ th reciprocal-lattice vector multiplied by  $2\pi$ , and  $\chi_{\omega}^{ij}(\mathbf{k}_0, \mathbf{k}_m)$  is the Fourier component of the complex tensor of crystal polarizability that can be calculated with due regard for all the processes of X-ray interaction with the crystal (for details, see [8, 9]).

Substituting (2) into (1), we arrive at an infinite system of equations for amplitudes  $\mathbf{E}(\mathbf{k}_m, \omega)$ . As a rule, all of the amplitudes  $\mathbf{E}(\mathbf{k}_m) \equiv \mathbf{E}_m$  are small in comparison with  $\mathbf{E}_0$ , because  $(\mathbf{k}_0^2 - K^2) \approx \chi_0 K^2$  and  $(\mathbf{k}_m^2 - K^2) = 2\mathbf{k}_0 \mathbf{h}_m + \mathbf{h}_m^2$  is of the order of  $K^2$ . Thus, the relationship  $\mathbf{E}_m / \mathbf{E}_0 \approx \chi_0 \approx 10^{-5}$  allows one to neglect all the scattered waves in comparison with  $\mathbf{E}_0$ . The situation is different if a crystal is oriented relative to the vector  $\mathbf{k}_0$  of the incident wave in such a way that the following condition is valid for the  $n$ th reciprocal-lattice vector:

$$(\mathbf{k}_n^2 - K^2) \approx \chi_0 K^2. \quad (3)$$

In this case, all of the amplitudes  $\mathbf{E}_0$  and  $\mathbf{E}_n$  become comparable, and one must solve the system of two vector equations. This is the case of two-beam diffraction with one diffracted beam.

One can readily see that, for any wavelength, condition (3) can readily be satisfied for two reciprocal-lattice vectors simultaneously (for example,  $n$ th and  $l$ th) with the aid of simple crystal rotations about two mutually perpendicular axes. In this case, there are two strong diffracted beams, and we arrive at three-beam diffraction. However, the real situation is even more complex. The simultaneous fulfillment of conditions  $\mathbf{k}_0^2 = \mathbf{k}_n^2 = \mathbf{k}_l^2 = K^2$  signifies that one can draw a circumference in the reciprocal lattice through three reciprocal-lattice points  $0, N$ , and  $L$ , which is a section of the Ewald sphere of radius  $K$ . In some cases, when the reciprocal lattice is of a high symmetry, the circumference can pass through more reciprocal-lattice points. Then, we arrive at four-, five-, or six-beam, etc. diffraction, respectively. An elegant method for determining these additional reciprocal-lattice points was described by Pinsker [1].

With due regard for the aforesaid, let us consider the case where condition (3) is performed for  $N - 1$  reciprocal-lattice points, i.e., the case of  $N$ -beam diffraction in a plane-parallel plate with the surface normal  $\mathbf{n}_0$ . Then the wave vector  $\mathbf{k}_0$  of an incident wave is expressed in terms of the wave vector  $\mathbf{K}_e$  of the wave in vacuum:  $\mathbf{k}_0 = \mathbf{K}_e + \varepsilon \mathbf{n}_0 / 2$ . Let us pass from the vector amplitudes of the electric field to scalar ones, using the decomposition

$$\mathbf{E}(\mathbf{k}_m) = \gamma_m^{-1/2} \sum_{s=\pi, \sigma} B_{ms} \mathbf{e}_{ms}, \quad (4)$$

where  $\mathbf{e}_{m\pi}$  and  $\mathbf{e}_{m\sigma}$  are mutually perpendicular unit vectors of polarization normal to  $\mathbf{k}_m$ , and  $\gamma_m = (\mathbf{k}_m \cdot \mathbf{n}_0) / K$ .

Then the system of  $2N$  self-consistent equations can be solved as a problem of eigenvalues of a certain matrix

$$\varepsilon B_{ms} = \sum_{m's'} K \gamma_m^{-1/2} \gamma_{m'}^{-1/2} (-\alpha_m \delta_{mm'}^{ss'} + \chi_{mm'}^{ss'}) B_{m's'}. \quad (5)$$

Here,  $\delta_{mm'}^{ss'}$  is the Kronecker symbol, and  $\alpha_m$  is the parameter characterizing the deviation of the  $m$ th reciprocal-lattice vector from the Bragg condition

$$\alpha_m = [(\mathbf{K}_e + \mathbf{h}_m)^2 - K^2] / K^2. \quad (6)$$

The matrix

$$\chi_{mm'}^{ss'} = \sum_{ij} e_{ms}^i \chi_{\omega}^{ij}(\mathbf{k}_m, \mathbf{k}_{m'}) e_{m's'}^j \quad (7)$$

consists of elements that represent the scattering amplitude of diffracted beams in the kinematical approximation. Therefore, hereinafter, their matrix is called the kinematical-scattering matrix.

Problem (5) has  $2N$  solutions. There are  $2N$  various three-dimensional configurations of the radiation wave field (i.e., of the X-ray standing waves). Each wave interacts with the crystal atoms in a different way and, in particular, is differently absorbed during its propagation through the crystal. The total amplitude of the electric field of an X-ray wave is the superposition of all the standing waves having different coefficients  $a_j$  (hereinafter called the excitation degrees). The values of these coefficients are determined from the boundary conditions on the entrance surfaces of the plate. Assume that the amplitudes of external beams form a vector  $\mathbf{D}_{ms} \gamma_m^{-1/2}$ . Then the system of equations for  $a_j$  can be written in the form

$$\sum_j B_{msj} \exp(i\varepsilon_j t_m / 2) a_j = \mathbf{D}_{ms}, \quad (8)$$

where  $t_m = 0$ , if  $\gamma_m > 0$ ;  $t_m = t$ , if  $\gamma_m < 0$ ; and  $t$  is the crystal plate thickness. Unknown amplitudes of the diffracted beams are

$$\mathbf{R}_{ms} = \sum_j B_{msj} \exp(i\varepsilon_j z_m / 2) a_j, \quad (9)$$

where  $z_m = t$ , if  $\gamma_m > 0$ ;  $z_m = 0$ , if  $\gamma_m < 0$ . The coefficient of the scalar-wave ( $ms$ ) reflection into the wave ( $m's'$ ) equals the squared modulus of the ratio of an unknown amplitude to the known one

$$P(m's', ms) = \left| \frac{R_{m's'}}{D_{ms}} \right|^2. \quad (10)$$

The boundary-value problem can readily be solved by the methods of matrix algebra. With this aim, we rewrite equations (5), (8), and (9) in the matrix form

$$\mathbf{B} * \varepsilon = \mathbf{G} * \mathbf{B}, \quad \mathbf{X} * \mathbf{A} = \mathbf{D}, \quad \mathbf{R} = \mathbf{Y} * \mathbf{A}, \quad (11)$$

where  $\varepsilon_{jj} = \varepsilon_j \delta_{jj}$  is the diagonal matrix of eigenvalues. Calculating the vector  $\mathbf{A}$  with the aid of the inverse matrix  $\mathbf{X}^{-1}$ , we obtain an unknown vector  $\mathbf{R}$  in the form

$$\mathbf{R} = \mathbf{Y} * \mathbf{X}^{-1} * \mathbf{D} = \mathbf{M} * \mathbf{D}, \quad \mathbf{M} = \mathbf{Y} * \mathbf{X}^{-1} \quad (12)$$

Thus, we arrived at a new matrix  $\mathbf{M}$  directly relating unknown amplitudes of the diffracted beams with the known amplitudes of the incident beams. The latter matrix is called the dynamical-scattering matrix.

In a conventional X-ray diffraction experiment, there is only one incident beam. But the situation is different if a crystalline plate is a layer of a multilayer crystalline system. Without going into detail, we would like to note that the exact solution of this complex problem was obtained by Kohn [10]. A similar situation can also arise in multicrystal systems.

### 3. X-RAY OPTICS OF A MULTIPLE-DIFFRACTION EXPERIMENT

Two main requirements for the incident beam should be met in order to observe dynamical effects in a conventional two-beam X-ray experiment. First, the angular intensity distribution should be narrower than the width of the intrinsic reflection curve of the crystal. This can readily be attained with the aid of an asymmetric crystal-collimator [11]. Second, the width of the spectral  $\Delta\lambda/\lambda$  distribution should be of the same order of magnitude or even narrower than the width of the intrinsic reflection curve. In a two-beam experiment, the fulfillment of the second condition is unnecessary if one uses a nondispersive arrangement where the diffracting planes of both the crystal-collimator and the specimen are parallel. This explains the widespread use in two-beam experiments of double- and multicrystal nondispersive arrangements with asymmetric crystals.

In multiple X-ray diffraction experiments, both of the above conditions should be met simultaneously for all the reflections. This makes it necessary to provide the angular collimation of the incident beam in several directions simultaneously. Thus, Greiser and Materlik [12] used a narrow slit to reduce the horizontal divergence of an SR beam in a three-beam (333/511) experiment. Collimation with the aid of an additional crystal was also used for solving the phase problem [13, 14]. The best angular collimation (0.5'' and 8.0'' in the horizontal and vertical planes, respectively) was attained with the use of mutually perpendicular asymmetric Si(111) crystal and channel-cut collimating Si(220) crystal [14]. However, the dispersion problem has not yet been solved.

In our experiments [5], we used two multicrystal arrangements, shown in Figs. 1 and 2, in the application of the method of X-ray standing waves. In the first arrangement (Fig. 1), the monochromatization of an SR beam from a bending magnet and its collimation in the vertical plane for the case of three-beam (111/220) diffraction was provided by a double-crystal monochromator with symmetric Si(111) crystals. Collimation in

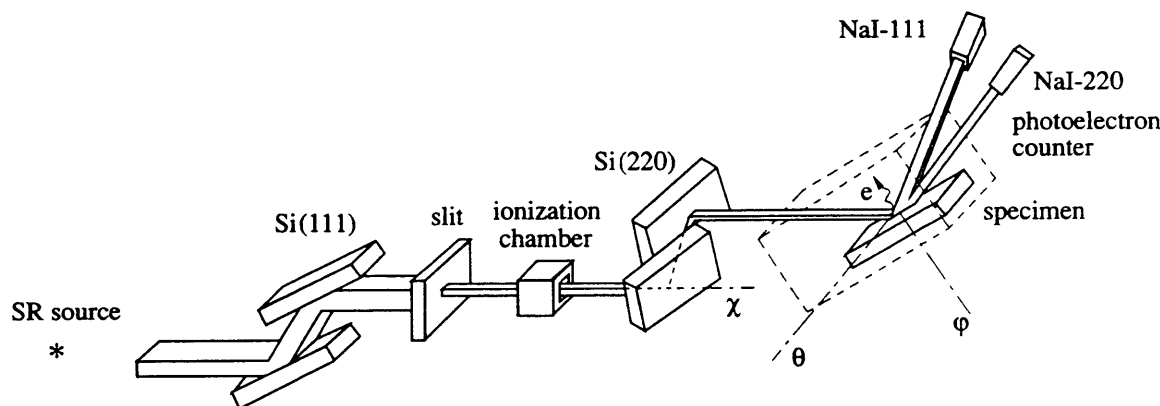


Fig. 1. X-ray optics of multiple diffraction experiments using a channel-cut crystal for two-dimensional collimation.

the horizontal plane was provided by a channel-cut Si(220) crystal with double reflection. To make the nondispersive arrangement, the channel-cut crystal was inclined in such a way that the (220) diffraction planes of the collimator and the specimen were parallel. This was provided by rotating a crystal for a necessary angle about the incident-beam direction. Thus, when processing experimental data, we could consider the angular divergence of the incident beam only. This divergence was determined as a product of the reflection curves  $R_{111}$  for a double-crystal monochromator and  $R_{220}$  for a channel-cut collimating crystal. On the two-dimensional ( $\theta$ ,  $\phi$ ) diagram, the intensity distribution of the incident beam is seen as the region of intersection of two bands (Fig. 8b). It is precisely this region that was used to calculate the convolution in processing the theoretical data and their comparison with the experimental results. Their perfect agreement [5] confirms the efficiency of the suggested arrangement.

However, the above approach is not universal. Therefore, it is very important to find a universal arrangement for collimation that can be used in various multibeam combinations. The most promising here is the use of multibeam effects themselves. In particular, it is well known [15] (see also Sect. 4) that the angular range of anomalously transmitted X-rays in six-beam diffraction is limited in two mutually perpendicular directions. The second X-ray optical arrangement (Fig. 2) is based on the use of this phenomenon.

An SR beam from a vertical wiggler is monochromatized with the aid of two symmetric Si(111) crystals and reflected by a Si(220) crystal toward the collimator and the specimen. The collimator is a 5-mm-thick Si(111) crystal positioned for a six-beam Laue diffraction. An anomalously transmitted direct beam is incident onto a crystal-specimen. We used this arrangement in both experiments on six-beam diffraction proper and in experiments on three beam (111/220) diffraction. Note that, in the general case, this arrangement is dispersive. However, as was shown earlier [5], a six-beam collimator provides an additional beam monochromatization up to  $\Delta\lambda/\lambda = 1.5 \times 10^{-5}$ . In three-beam (111/200) diffraction, this value is much lower than the angular ranges of the

reflections under study. Therefore, it is possible to ignore the incomplete monochromatization and to consider only angular beam divergence.

Concluding this section, we would like to note that the second arrangement is fundamentally new, and we were the first to use it. However, the variety of possible X-ray optical arrangements for multiple diffraction experiments is not limited to the cases considered above. On the other hand, the modified methods of two-dimensional angular collimation can also be used successfully in other fields of X-ray diffraction (such as diffraction under the conditions of total external reflection, topography, etc.)

#### 4. ANOMALOUS TRANSMISSION OF X-RAYS IN SIX-BEAM DIFFRACTION

The phenomenon of anomalous transmission of X-rays through a thick absorbing crystal under the conditions of two-beam diffraction was first discovered by Borrmann in 1941 [16]. Since then, the phenomenon has been studied in detail both theoretically and experimentally. Physically, the effect consists in excitation in a crystal of a standing-wave field whose intensity is modulated along the diffraction vector and is close to zero at the reflecting planes. A more complex structure of the wave field under the conditions of multiple diffraction allows one to suppress the interaction of the X-ray radiation with crystal atoms.

Here six-beam (220, 242, 044,  $\bar{2}24$ ,  $\bar{2}02$ ) diffraction where twelve Bloch waves are excited in a crystal (six for each polarization state) is of great interest. Each of these waves is characterized by its own absorption coefficient. The structure of the most weakly absorbed field is such that not only the amplitudes of the field, but also its first and second derivatives, with respect to coordinates, are zero at the crystal lattice points. As a result, photoelectric absorption is substantially suppressed; therefore, the minimum absorption coefficient is limited by Compton scattering alone [17, 18].

The unique properties of six-beam diffraction attracted the attention of many researchers (see the references in [1, 7]). The simplest experimental arrange-

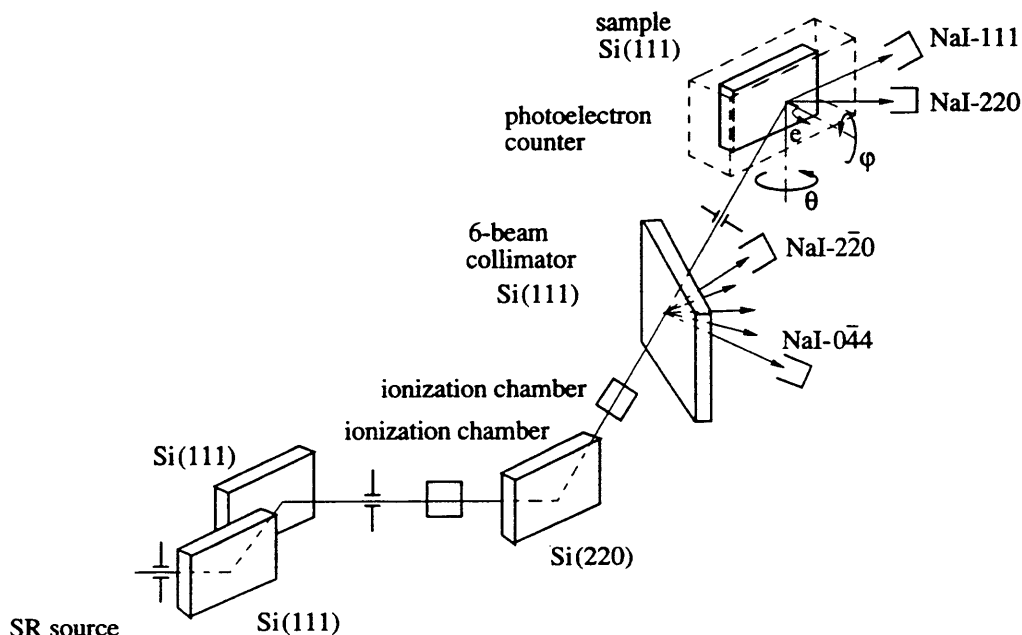


Fig. 2. The arrangement of a multiple X-ray diffraction experiment with a six-beam collimator.

ment was used when the lines of anomalous transmission were recorded on photographic plates. Theoretical analysis of the experimental results showed [19, 20] that, in this case, the effect of anomalous transmission is masked by the optical effects of focusing and defocusing. The latter makes the quantitative studies of anomalous transmission almost impossible. Thus, the only method possible here is direct intensity measurements of the transmitted beam in the diffractometric experiment. Such measurements were first performed only recently, with the use of synchrotron radiation [2].

The schematic diagram of the experiment is shown in Fig. 3. The specific features of a six-beam collimator were considered in Sect. 3. We note here only that the above effect was used in hopes of attaining angular collimation sufficient for studying the effect itself.

The specimens were dislocation free 3- and 5-mm-thick Si crystals. We measured the  $\Delta\theta$ -dependences of the transmitted beam intensity for various values of  $\Delta\phi$ . The measurements were made at the wavelengths  $\lambda = 0.93$  and  $1.15 \text{ \AA}$ , corresponding to  $\mu t = 12$  and  $24$ , for a crystal of thickness  $t = 3 \text{ mm}$ , and to  $\mu t = 19.4$  and  $39.7$ , for a crystal with  $t = 5 \text{ mm}$ .

Figure 4 shows the experimental two-dimensional intensity distribution for a transmitted beam for  $\mu t = 12$ . The value  $\Delta\phi = 0$  corresponds to the center of the six-beam region. A relatively low value of  $\mu t$  allows one to observe the intensity distribution both inside and outside the six-beam region and to compare in detail the experimental and calculated results. As is evident from Fig. 4, the peak intensity in the center of the six-beam region is more than three times higher than the intensity of the 220 peaks. This indicates the enhancement of anomalous transmission, although it is weakly marked for the given value of  $\mu t$ .

In order to compare the experimental and theoretical data, we calculated the transmission coefficients  $P(0p, 0s, \Delta\theta, \Delta\phi)$  defined as the intensity ratios of the  $p$ -polarized plane wave in the direct beam at the exit surface to the intensity of the  $s$ -polarized wave at the entrance surface of the crystal [see formula (10)]. With due regard for the notation introduced in Sect. 2, these coefficients can be calculated by the formula

$$P(0p, 0s, \Delta\theta, \Delta\phi) = \sum_j [B_{0pj} B_{0sj}]^2 \exp(-\mu_j t). \quad (13)$$

In our case of pure Laue geometry, the calculations can be simplified almost without any loss in accuracy by using the approximation in which problem (5) is solved for a nonabsorbing crystal, i.e., in the zeroth order with respect to  $\chi_i/\chi_r$ . The absorption coefficients  $\mu_j$  for each standing-wave field are calculated in the first approximation as the diagonal elements of the absorption matrix

$$\mu_j = \sum_{mp} \sum_{ns} B_{mpj} [K\gamma_m^{-1/2} \gamma_n^{-1/2} \chi_{imn}^{ps}] B_{nsj}. \quad (14)$$

Figure 5 shows the calculated two-dimensional intensity distribution for a transmitted beam for a  $\sigma$ -polarized incident plane wave (the so-called intrinsic curves). One can clearly see five intersecting bands corresponding to different angular ranges of the two-beam Borrmann effect. The bands corresponding to weak reflections are narrower, but the transmission maximum is rather high because of a low  $\mu t$  value. The experimental curves show no peaks due to weak reflections because of insufficient collimation of the incident beam. To be able to compare the theoretical and experimental

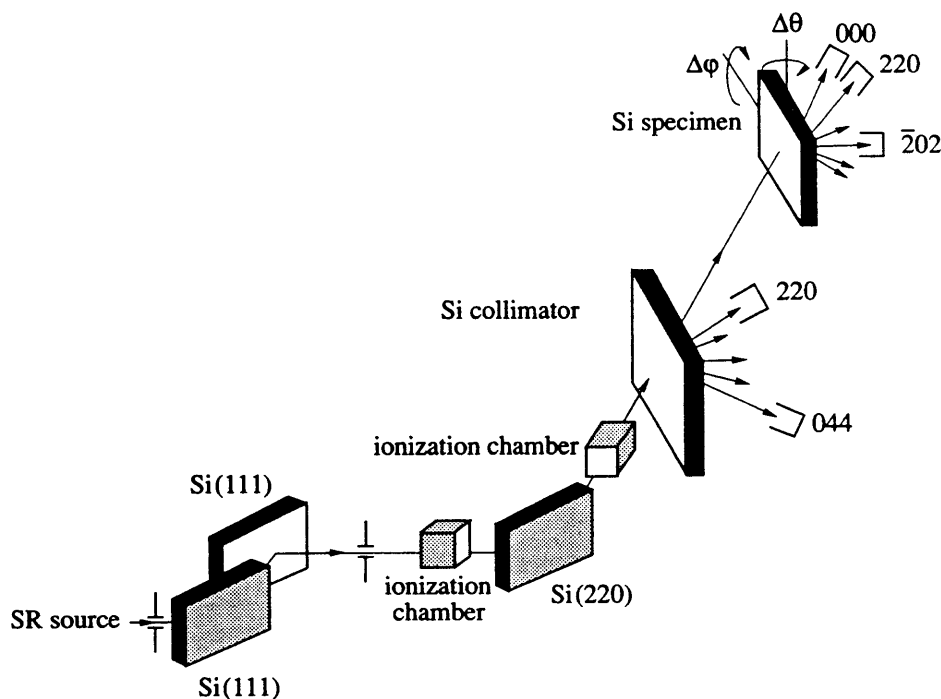


Fig. 3. Schematic diagram of an X-ray experiment for studying anomalous transmission under the conditions of six-beam diffraction.

data, one must calculate the two-dimensional convolution of the transmission coefficient for a specimen with the transmission coefficient  $P_c(s, \sigma, \Delta\theta, \Delta\phi)$  for a six-beam collimator. The convolution is calculated as

$$I(\Delta\theta, \Delta\phi) = \left( \sum_{p, s, R} \int d\xi d\eta P(0p, 0s, \Delta\theta + \xi, \Delta\phi + \eta) \times P_c(s, \sigma, \xi, \eta) \right) \times \left( \sum_s \int_R d\xi d\eta P_c(s, \sigma, \xi, \eta) \right)^{-1} \quad (15)$$

and takes into account the change in the polarization state of the incident  $\sigma$ -polarized SR beam upon its transmission through the crystal-collimator. The angular range  $R$  used in the calculations makes an essential effect on averaging. However, if one considers that the radiation is not completely monochromatic, and therefore, its angular range is not known exactly, the angular range is assumed to be somewhat wider than follows from the preliminary collimation of the monochromatic radiation. This problem occurs only for low  $\mu t$  values.

Figure 6 shows the theoretical and experimental curves for three  $\Delta\phi$  values. The sufficiently good agreement between the theory and the experiment confirms the efficiency of the suggested experimental approach to the quantitative study of anomalous transmission in six-beam diffraction. A more pronounced effect of anomalous transmission can be observed only at higher  $\Delta\phi$  values. The respective analysis of this case will be performed in the near future.

### 5. THE METHOD OF X-RAY STANDING WAVES UNDER THE CONDITIONS OF MULTIBEAM DIFFRACTION

The method of X-ray standing waves is used to measure, along with the intensities of diffracted beams, the intensity of inelastic-scattering channels (secondary processes). Theoretically, the calculation of the latter reduces to the following [21, 22]: first, the intensity of the total radiation field is calculated at a certain point  $\mathbf{r}$  in the vicinity of the position of an atomic nucleus  $\mathbf{r}_A$  located at the depth  $z$ :

$$F(\mathbf{r}) = \left| \sum_m \mathbf{E}(\mathbf{k}_m) \exp(i\mathbf{k}_m \mathbf{r}) \right|^2 \quad (16)$$

$$= \sum_{mn} \mathbf{E}_m^*(z) \mathbf{E}_n(z) \exp [i(\mathbf{h}_n - \mathbf{h}_m) \mathbf{r}] .$$

The phase factor should be averaged with due regard for the electron density distribution of the atom and the probability of inelastic processes and thermal vibrations.

Then the result can be written in the form

$$I_s(z) = \langle F(\mathbf{r}) \rangle = \sum_m |\mathbf{E}_m(z)|^2 + \sum_{mn} \mathbf{E}_m^*(z) \mathbf{E}_n(z) \frac{\chi_{imn}(s)}{\chi_{i00}(s)} . \quad (17)$$

The prime at the sum sign indicates that the term with  $m = n$  is eliminated; and  $\chi_{imn}(s)$  describes the contribution of the X-ray absorption process denoted by  $s$ , to the imaginary part of the Fourier component of polarizabil-

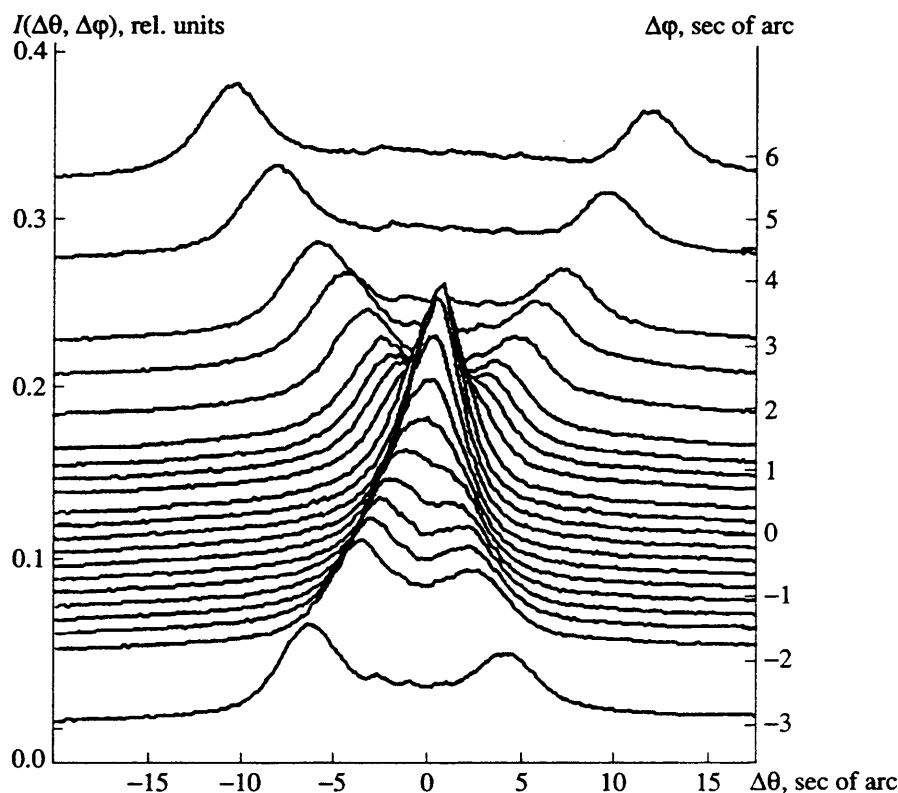


Fig. 4. The experimental two-dimensional distribution ( $\Delta\theta$ ,  $\Delta\phi$ ) of the transmission coefficient under the conditions of six-beam diffraction.

ity. Finally, in order to calculate the intensity of the secondary-radiation yield from the crystal, the result should be integrated over the crystal depth with due regard for the probability  $P_s(z)$  of the secondary radiation yield

$$I_{SR}^s = \int_0^t dz P_s(z) I_s(z). \quad (18)$$

If one measures photoelectron emission from the entrance surface of the crystal in the Bragg (reflection) diffraction, the escape depth of the secondary radiation is much less than the depth of reflection, whereas the polarizability ratio is close to unity. Then, the angular dependence of the secondary process reflects the angular dependence of the intensity of the X-ray wave field at the point of the atom location in the subsurface crystal layer

$$I_{ph} \approx \left| \sum_m \mathbf{E}_m(0) \right|^2. \quad (19)$$

If the atom is displaced from its position in the lattice or if the lattice points in the subsurface layer are displaced with respect to those of the matrix in which the X-ray standing waves are formed, then the formula becomes

$$I_{ph} \approx \left| \sum_m \mathbf{E}_m(0) \exp [i \mathbf{h}_m \mathbf{u}(0)] \right|^2. \quad (20)$$

The additional phase factors, considering the displacements of atoms, drastically change the character of the angular dependence, which, unlike that in the two-beam case, is sensitive to two coordinates of the displacement in the plane of the reciprocal-lattice vectors. This provides the two-dimensional localization of atoms in the surface layer.

Greizer and Materlik [12] studied the fluorescence yield from a Ge crystal under the conditions of three-beam (511/333) diffraction. We measured the yield of photoelectrons excited by an X-ray standing wave under the conditions of three-beam (111/220) diffraction [3, 6]. The specimen was a perfect Si(111) crystal. The yield of *K*-photoelectrons was measured by a gas-proportional counter [23] specially designed for multi-beam measurements and for providing rotation of a crystal with a sufficient accuracy about the  $\phi$ -axis perpendicular to the surface in the vacuum-tight counter.

Figure 7 shows the yield curves and the curves for (111) and (220) reflection measured in the central part of the three-beam diffraction region at different values of the azimuth angle  $\Delta\phi$  (the point  $\Delta\theta = \Delta\phi = 0$  corresponds to the center of the three-beam region). The escape depth of photoelectrons is very small ( $\approx 0.2 \mu\text{m}$ ); therefore, the photoemission curves demonstrate quite clearly the interference of the wave fields in the crystal. Thus, the yield of photoelectrons substantially decreases in the region of total external reflection corresponding to the left-hand parts of

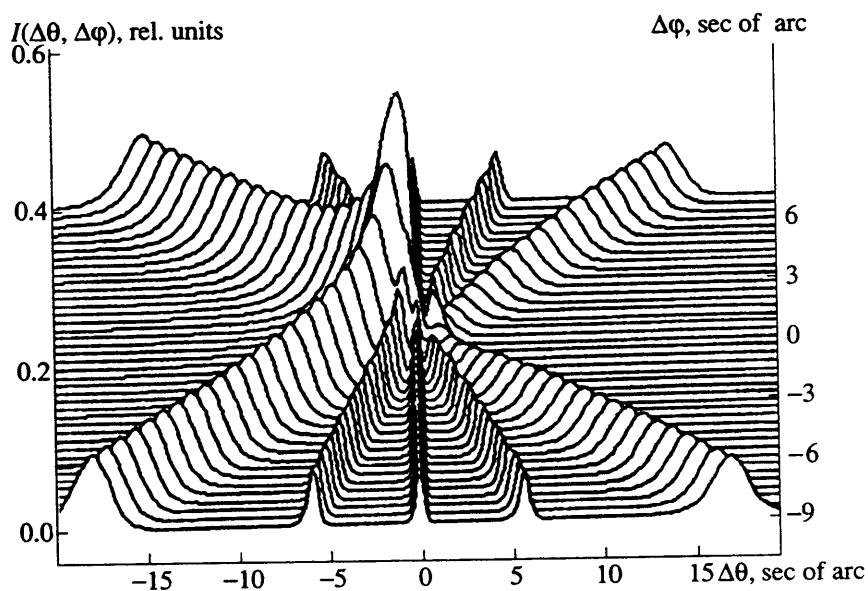


Fig. 5. Theoretically calculated two-dimensional ( $\Delta\theta$ ,  $\Delta\phi$ ) distribution of the transmission coefficient for a  $\sigma$ -polarized plane wave under the conditions of six-beam diffraction.

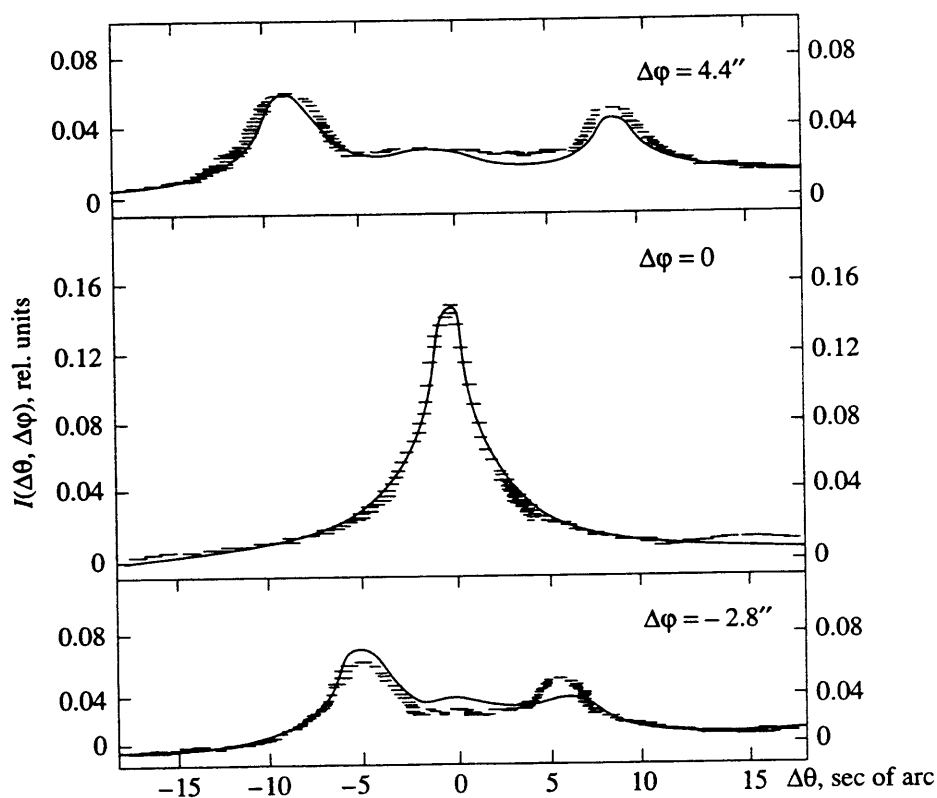


Fig. 6. Comparing the experimental (dashed line) and theoretically calculated (solid lines) transmission coefficients with due regard for the two-dimensional convolution.

the curves in Fig. 7 (for the 220 curves, at  $\Delta\phi < 0$ ; for the 111 curves, at  $\Delta\phi > 0$ ). On the other hand, if the condition of the three-beam diffraction (Fig. 7c) is fulfilled exactly, the photoelectron yield exceeds the respective value for two-beam diffraction by a factor of 1.5.

One of the advantages of the multibeam arrangement for the X-ray standing-wave method is the possibility of measuring the yield curves for several reflections, in fact, under the conditions of two-beam diffraction. Figure 7f shows the angular dependence of the

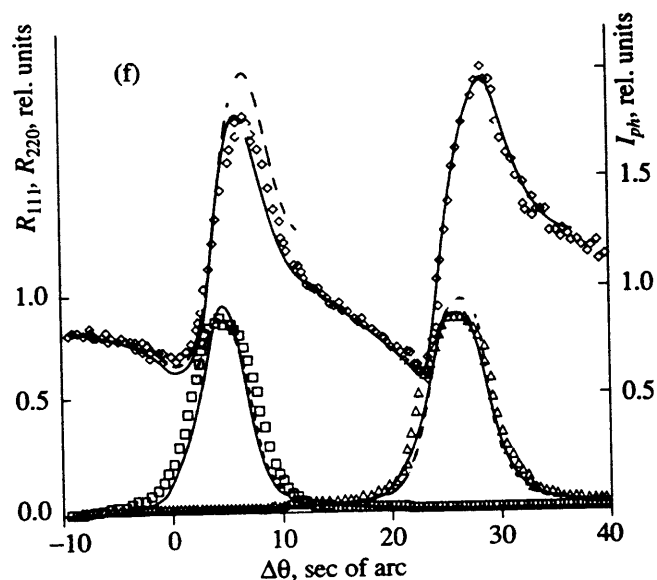
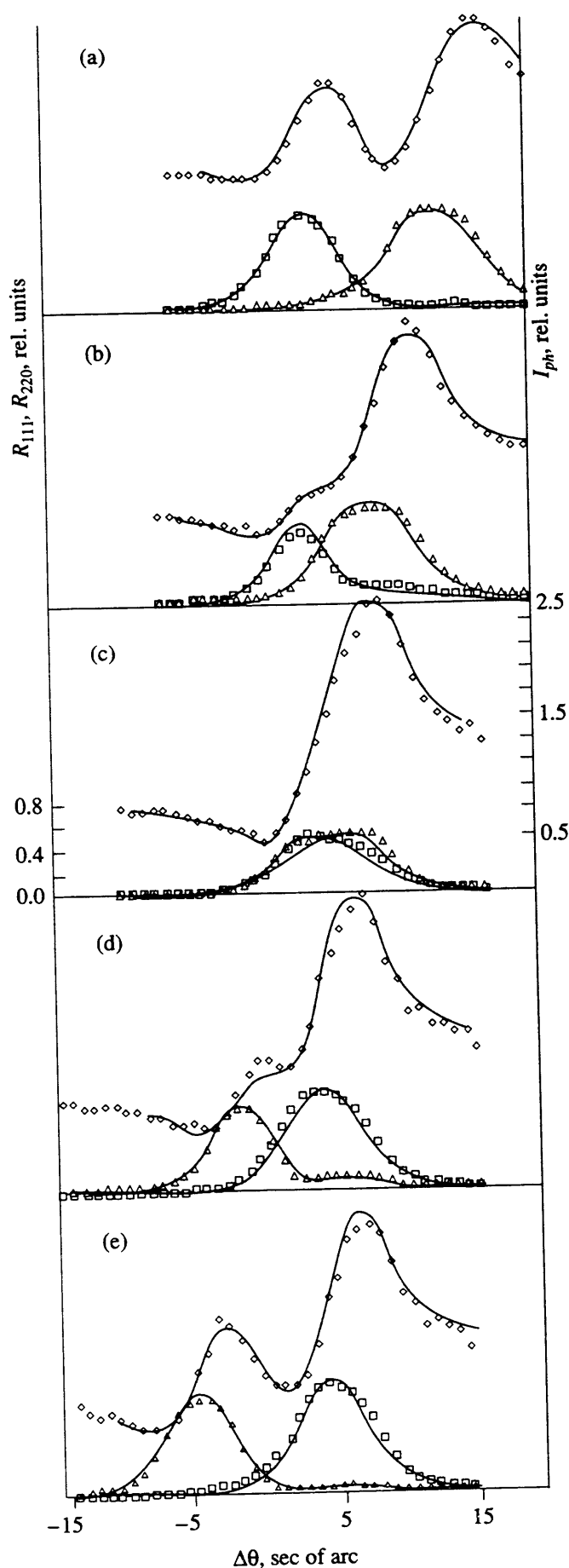


Fig. 7. The curves of photoelectron yield (rhombs) and the ( $111$ ) (squares) and ( $220$ ) (triangles) reflection curves under the conditions of three-dimensional  $111/220$  diffraction for various angles  $\Delta\phi$ : (a)  $-12.8''$ , (b)  $-7''$ , (c)  $-0.5''$ , (d)  $5.3''$ , and (e)  $12''$ ; (f) the same data outside the region of strong interactions ( $\Delta\phi = 30''$ ). The dashed line shows the data calculated by the two-beam theory.

photoelectron yield and the reflection curves for a rather pronounced deviation from the exact three-beam position ( $\Delta\phi = 30''$ ). The experimental curve obtained agrees quite well with the curves calculated by the two-beam theory. Obviously, an increase of the angle  $\Delta\phi$  makes the two-beam approximation more accurate. Thus, in one angular scan, one can measure the curves of secondary processes for several reflections. This is especially useful when one has to study structural changes occurring with time.

## 6. RECORDING OF PHASE-SENSITIVE CURVES BY THE METHOD OF THREE-BEAM DIFFRACTION

Three-beam diffraction allows one to implement a situation close to that in the two-beam X-ray standing wave method but without measuring secondary processes. Such a situation arises when the Bragg condition (3) is fulfilled rigorously for the first beam  $H$ , whereas, for the second beam  $G$ , it is fulfilled only approximately. In this case, the beam  $G$  can be considered in the kinematical approximation. Producing no effect on the strong beams  $0$  and  $H$ , the beam  $G$  itself is generated by the coherent superposition of these strong beams. Therefore, the angular dependence of  $G$  is formed under a strong influence of the angular dependence of the reflection-amplitude phase. In turn, this fact allows one to measure the phase of the structure factor, in other words, to solve the phase problem of the structure analysis directly. This was first demonstrated in [14].

In actuality, the analogy of this method with the method of X-ray standing waves is even closer. As was

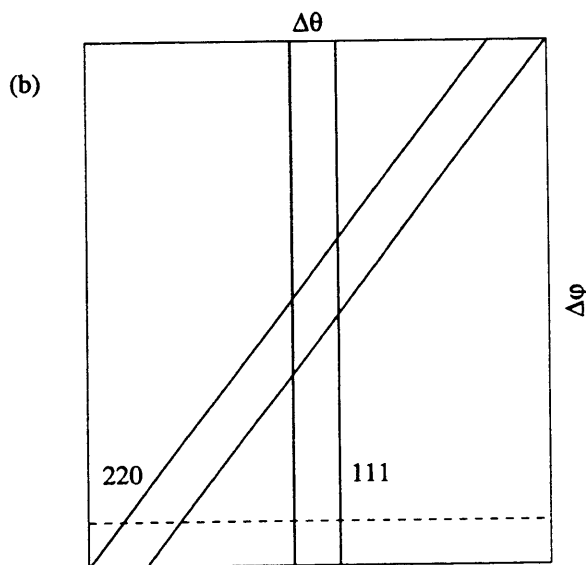
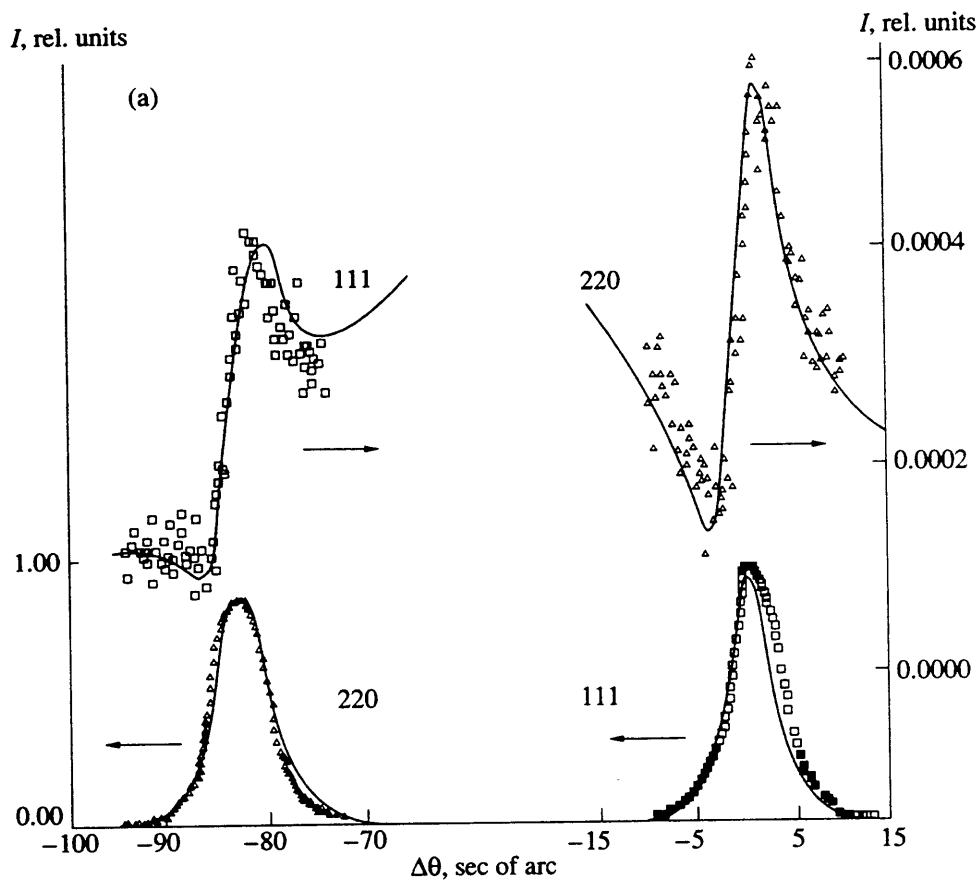


Fig. 8. (a) The angular dependences of the intensities at the tails of the (111) and (220) reflection curves in the angular regions of the total (220) and (111) reflections, respectively. (b) Mutual arrangement of the reflection regions on the  $(\Delta\theta, \Delta\phi)$  diagram. The dashed line corresponds to  $\Delta\theta$ -scanning.

shown earlier [10, 22, 24], this method proved to be very convenient for studying the structure of subsurface layers, because a weak beam is formed in the vicinity of the surface, and the depth of its reflection is inversely proportional to the deviation from the Bragg angle in

full analogy with the well-known method of asymptotic diffraction [25]. Even if the deviation angle is quite small, the effective depth of reflection is smaller than the escape depth of photoelectrons, and, therefore, one can use the approximation of the zero reflection depth.

In this approximation, the intensity of a weak  $G$  beam is determined to be

$$I_{gs}(z) \approx \sum_{p=\pi, \sigma} (\mathbf{e}_{gp} \mathbf{e}_{0s})^2 \times \left| \mathbf{E}_{0s}(0) + \mathbf{E}_{hs}(0) \frac{\chi_{gh}^{ps}}{\chi_{g0}^{ps}} \exp[-i\mathbf{h}\mathbf{u}(0)] \right|^2 \quad (21)$$

Here, notation (7) is used:  $s$  is the index of two-wave polarization for beams 0 and  $H$ , and  $p$  is the polarization index for the beam  $G$  polarization. As follows from formula (21), the anomalous angular dependence can be observed only if all three of the reflections are not forbidden.

Up to now, no experimental studies of the structure of disturbed surface layers have been performed using this method. For perfect crystals, a large number of various methods for direct determination of structure factors are known. The diffractometric method analogous to the one described above was first applied in [14], where the authors used a conventional X-ray tube. The anomalous angular dependences similar to the photoemission curves were first recorded with the use of SR and the new collimation method described in Sect. 3 in our study [4].

The experiment was performed on a Si(111) crystal for the three-beam case (111, 220). The angular dependence of both beams obtained in two-beam regions of the total reflection is shown in Fig. 8a for the deviation from the exact three-beam condition  $\Delta\varphi = -115''$ . The upper curves correspond to weak beams with anomalous angular dependence; the lower curves correspond to strong beams, with the reflection coefficient close to unity. The solid curves were calculated by the exact formula of multiple diffraction with due regard for the convolution with the curves of intensity distribution for the crystal-collimator. Figure 8b shows the two-dimensional ( $\Delta\theta, \Delta\varphi$ ) diagram illustrating the location of the (111) and (220) regions of total reflection and the line of  $\Delta\theta$ -scanning (dashed line). These curves demonstrate, first, the phase-sensitive nature of the angular dependence of weak beams and, second, the exact correspondence of the obtained experimental data to the respective theoretical calculations. (Note that no detailed comparison with the theoretical predictions was made in [14].) Thus, we believe that the above suggested procedure can be used as a new method for structure diagnostics of slightly disturbed subsurface layers.

#### REFERENCES

1. Pinsker, Z.G., *Rentgenovskaya Kristallooptika*, Moscow: Nauka, 1982; *Dynamical Scattering of X-rays in Crystals*, Berlin: Springer, 1984.
2. Kazimirov, A.Yu., Kovalchuk, M.V., Kohn, V.G., Ishikawa, T., and Kikuta, S., *Photon Factory Activity Report*, 1991, vol. 9, p. 238.
3. Kazimirov, A.Yu., Kovalchuk, M.V., Kohn, V.G., Kharitonov, I.Yu., Samoiloa, L.V., Ishikawa, T., and Kikuta, S., *Photon Factory Activity Report*, 1991, vol. 9, p. 239.
4. Kazimirov, A.Yu., Kovalchuk, M.V., Kohn, V.G., Kharitonov, I.Yu., Samoiloa, L.V., Ishikawa, T., and Kikuta, S., *Photon Factory Activity Report*, 1991, vol. 9, p. 240.
5. Kazimirov, A.Yu., Kovalchuk, M.V., Kharitonov, I.Yu., Samoiloa, L.V., Kikuta, S., and Ishikawa, T., *Rev. Sci. Instrum.*, 1992, vol. 63, no. 1, p. 1019.
6. Kazimirov, A.Yu., Kovalchuk, M.V., Kohn, V.G., Kharitonov, I.Yu., Samoiloa, L.V., Ishikawa, T., and Kikuta, S., *Phys. Status Solidi A*, 1993, vol. 135, p. 507.
7. Chang, Shih-Lin, *Multiple Diffraction of X-rays in Crystals*, Berlin: Springer, 1984.
8. Afanas'ev, A.M. and Kagan, Yu., *Acta Crystallogr., Sect. A: Found. Crystallogr.*, 1968, vol. 24, no. 1, p. 163.
9. Kolpakov, A.V., Bushuev, V.A., and Kuz'min, R.N., *Usp. Fiz. Nauk*, 1978, vol. 126, no. 3, p. 479.
10. Kohn, V.G., *J. Moscow Phys. Soc.*, 1991, vol. 1, no. 4, p. 425.
11. Renninger, M., *Z. Naturforsch.*, 1961, vol. 160, p. 1110; Kohra, K., *J. Phys. Soc. Jpn.*, 1962, vol. 17, p. 1322.
12. Greiser, N. and Materlik, G., *Z. Phys. B: Condens. Matter*, 1987, vol. 66, p. 83.
13. Post, B., Nicolosi, J., and Ladell, J., *Acta Crystallogr., Sect. A: Found. Crystallogr.*, 1984, vol. 40, p. 684.
14. Kov'ev, E.K. and Simonov, V.I., *Pis'ma Zh. Eksp. Teor. Fiz.*, 1986, vol. 43, p. 244.
15. Kohn, V.G., *Fiz. Tverd. Tela* (Leningrad), 1976, vol. 18, p. 2538.
16. Borrmann, G., *Z. Phys.*, 1941, vol. 42, p. 157.
17. Afanas'ev, A.M. and Kohn, V.G., *Acta Crystallogr., Sect. A: Found. Crystallogr.*, 1977, vol. 33, p. 178.
18. Kohn, V.G., *Kristallografiya*, 1987, vol. 32, p. 844.
19. Kohn, V.G., *Fiz. Tverd. Tela* (Leningrad), 1977, vol. 19, p. 3567.
20. Kohn, V.G. and Toneyan, A.H., *Acta Crystallogr., Sect. A: Found. Crystallogr.*, 1986, vol. 42, p. 441.
21. Kohn, V.G., *Fiz. Tverd. Tela* (Leningrad), 1986, vol. 28, p. 3028.
22. Kohn, V.G., *Phys. Status Solidi A*, 1988, vol. 106, p. 31.
23. Koval'chuk, M.V., Nikolaenko, A.M., Semiletov, A.S., Kharitonov, I.Yu., and Shilin, Yu.N., *Prib. Tekh. Eksp.*, 1991, no. 3, p. 176.
24. Kohn, V.G. and Samoiloa, L.V., *Phys. Status Solidi A*, 1992, vol. 133, p. 9.
25. Afanas'ev, A.M., Aleksandrov, P.A., and Imamov, R.M., *Rentgenodifraktsionnaya Diagnostika Submikronnykh Sloev* (X-Ray Diffraction Diagnostics of Submicron Layers), Moscow: Nauka, 1989.